water

MDPI

Article

Chemodiversity and Molecular Mechanism Between Per-/Polyfluoroalkyl Substance Complexation Behavior of Humic Substances in Landfill Leachate

Jia Li [1,†], Haoqun Sha [2,†], Rongchuan Ye [3], Peipei Zhang [4], Shuhe Chen [2], Ganghui Zhu [1,*] and Wenbing Tan [2,*]

[1] Technical Centre for Soil, Agriculture and Rural Ecology and Environment, Ministry of Ecology and Environment, Beijing 100012, China; lijia@tcare-mee.cn
[2] State Environmental Protection Key Laboratory of Simulation and Control of Groundwater Pollution, Chinese Research Academy of Environmental Sciences, Beijing 100012, China; shahaoqun@126.com (H.S.)
[3] School of Chemical and Environmental Engineering, China University of Mining and Technology (Beijing), Beijing 100083, China
[4] College of Biological Science and Biotechnology, Beijing Forestry University, Beijing 100083, China
* Correspondence: zhuganghui@tcare-mee.cn (G.Z.); wenbingtan@126.com (W.T.)
† The authors contributed equally to this work.

Abstract: Landfill leachate contains a range of organic and inorganic pollutants, including per-/polyfluoroalkyl substances (PFASs), which can infiltrate into surrounding soil and groundwater through leaching processes, and can pose a threat to human health via food chains and drinking water processes. Thus, the transport of PFASs in landfill leachate is a research hotspot in environmental science. This study investigates the complexation and adsorption mechanisms between humic substances and PFASs in landfill leachate at the molecular level. Experimental results demonstrate that the binding constant $logK_{sv}$ of humic substances with PFASs correlates positively with specific ultraviolet absorbance ($SUVA_{254}$), absorbance ratio (A_{250}/A_{365}), humification index (HIX), and fluorescence index (FI), while it exhibits a negative correlation with the biological index (BIX). These findings indicate that high aromaticity is a prerequisite for molecular interactions between humic substances and PFASs, with polar functional groups further facilitating the interaction. Molecular-level analysis revealed that humic substances undergo complexation and adsorption with PFASs through hydrophobic interactions, van der Waals forces, hydrogen bonding, ionic bonding, and covalent bonding, by functional groups such as hydroxyl, aliphatic C-H bonds, aromatic C=C double bonds, amides, quinones, and ketones. Future efforts should focus on enhanced co-regulation and mitigation strategies addressing the combined pollution of PFASs and humic substances in landfill leachate.

Keywords: molecular mechanism; per-/polyfluoroalkyl substances (PFASs); landfill leachate; humic substances; complexation

check for updates

Citation: Li, J.; Sha, H.; Ye, R.; Zhang, P.; Chen, S.; Zhu, G.; Tan, W. Chemodiversity and Molecular Mechanism Between Per-/Polyfluoroalkyl Substance Complexation Behavior of Humic Substances in Landfill Leachate. *Water* **2024**, *16*, 3527. https://doi.org/10.3390/w16233527

Academic Editor: Christos S. Akratos

Received: 5 November 2024
Revised: 4 December 2024
Accepted: 5 December 2024
Published: 7 December 2024

1. Introduction

The environmental behavior and toxicity of per- and polyfluoroalkyl substances (PFASs) have garnered significant attention from researchers worldwide, becoming a major focus in environmental science research [1,2]. Unlike most organic pollutants, PFASs are highly water-soluble and mobile, leading to their widespread detection in various environmental media and biota globally [3,4]. Studies have shown that certain PFASs exhibit hepatotoxicity, immunotoxicity, and reproductive toxicity, with potential to cause endocrine disruption and teratogenic effects in organisms [5–8]. Landfills, a primary method of global urban solid waste disposal, represent a significant source of PFAS pollution in the environment [9,10]. PFAS transport within landfills primarily involves dissolution from solid waste into leachate, potentially contaminating groundwater, or entering the atmosphere via volatile gasses or particles, ultimately posing health risks to humans through drinking water and food chains [11,12].

The release of PFASs from solid waste in landfills into leachate is influenced by interactions with various substances present in the leachate, among which PFAS interactions with organic matter are particularly complex. Dissolved organic matter (DOM) comprises over 85% of the total organic content in leachate and plays a crucial role in PFAS behavior [13]. Humic substances, a primary component of DOM, contains various reactive groups, including carboxyl, hydroxyl, phenolic hydroxyl, and alcoholic hydroxyl groups [14]. Research indicates that the transfer of PFASs from solid to liquid phases in the environment is substantially influenced by the reactive groups and high organic content of humic substances [15]. In landfill leachate, the complexation and adsorption of PFASs by humic substances may facilitate the release of PFASs from solid waste into leachate, leading to the further transport of PFASs into surrounding environments. Therefore, the interaction mechanisms between PFASs and humic substances in leachate are critical in determining the transport of PFASs, which consequently pose human health and environmental risks. Understanding the complexation and adsorption mechanisms of humic substances on PFASs is essential for predicting PFAS transport in landfill leachate more accurately.

This study investigates the chemodiversity and molecular complexation characteristics between PFASs and humic substances by designing complexation experiments. By analyzing the chemodiversity characteristics of different humic substances in leachate and employing quenching models to evaluate complexation behavior, this research provides scientific support for a more comprehensive understanding of the molecular mechanism between PFASs and humic substances in municipal landfill leachate.

2. Materials and Methods

2.1. Reagents and Materials

Two categories of humic substances (humic acid and fulvic acid) were extracted from landfill leachate. Target PFAS standards and corresponding isotopic markers were purchased from Wellington Laboratories, Canada. The target PFAS standards included Perfluoro-n-butanoic acid (PFBA) and Perfluorobutanesulfonic acid (PFBS), with corresponding isotopically labeled internal standards $_{13}C_4$ PFBA and $_{18}O_2$ PFHxS. The primary reagents used in this experiment included NaOH, HCl, and $NaHCO_3$.

2.2. Sample Collection

Leachate samples were collected from 16 landfills in the Beijing–Tianjin–Hebei region of China, specifically from the following sites: Lixian (LX), Xiongxian (XX), Beijing Huafeng (BJH), Dacheng (DChe), Beijing Dongnanzhao (BJD), Dachang (DCha), Bazhou (BZ), Laishui (LX), Xianghe (XH), Zhuozhou (ZZ), Sanhe (SH), Baoding Wuhua (BDW), Tianjin Quantai (TJQ), Baoding Yuefeng Kewei (BDY), Wen'an Runda (WAR), and Wen'an Jielv (WAJ). Detailed landfill site information with landfill age, operation status, volume, and etc. is provided in Table S1. Leachate samples were collected from the end of the landfill drain and stored at 4 °C in the laboratory for analytical testing purposes. Each landfill collected 2 L of landfill leachate.

2.3. Solution Preparation

2.3.1. Humic Acid Solution

To prepare the humic acid (HA) solution, solid HA extracted from landfill leachate was added to a 0.1 mol/L NaOH solution (pH 11) and sonicated for 15 min until fully dissolved (this may require several hours). The resulting concentration of the HA stock solution was 1 g/L. The solution was filtered through a 0.45 μm membrane to obtain the supernatant, after which the pH was adjusted to 8 using HCl (slowly and with thorough mixing to prevent localized concentration effects and possible HA precipitation). HCl concentration was adjusted from 1 mol/L to 0.1 mol/L as needed. The HA solution was then diluted to 10 mg C/L and dispensed into 200 mL reagent bottles, with three parallel samples for each group.

2.3.2. Fulvic Acid Solution

To prepare the fulvic acid (FA) solution, solid FA extracted from landfill leachate was added to pure water and sonicated for 15 min to reach a concentration of 1 g/L. The FA solution was then diluted to 10 mg C/L and dispensed into 200 mL reagent bottles, with three parallel samples for each group.

2.4. Quenching Titration

2.4.1. HA Titration

PFBS was titrated into HA solutions to achieve a final concentration range of 0–100 µmol/L (0, 10, 50, 100 µmol/L). The pH of the system was maintained at 8.00 ± 0.05 using $NaHCO_3$ buffer solution, with the total amount of acid and base added not exceeding 100 µL. Similarly, PFBA was titrated into HA solutions to reach the same concentration range, with the same pH control and buffer solution additions as above (see Table S2). In the following, D1PS is used to represent HA and PFBS experimental groups, and D1PA is used to represent HA and PFBA experimental groups. Following titration, the reaction solution was shaken in darkness at a constant temperature of 25 °C for 24 h to allow the complexation reaction to reach equilibrium. Afterward, 200 mL of the reaction solution was freeze-dried to obtain the powdered complex, and the remaining solution was refrigerated for subsequent FTIR analysis.

2.4.2. FA Titration

PFBS was titrated into FA solutions to reach a final concentration range of 0–100 µmol/L (0, 10, 50, 100 µmol/L). The pH was maintained at 8.00 ± 0.05 with $NaHCO_3$ buffer solution, with total acid and base addition limited to 100 µL. Likewise, PFBA was titrated into FA solutions to reach the same concentration range, with the same pH adjustment as above (see Table S2). In the following, D2PS is used to represent the FA and PFBS test groups, and D2PA is used to represent the FA and PFBA test groups. Post-titration, the reaction solution was shaken at 25 °C in the dark for 24 h to reach complexation equilibrium. Following this, 200 mL of the reaction solution was freeze-dried to obtain the powdered complex, while the remaining solution was stored at 4 °C for further FTIR analysis.

2.5. Spectroscopic Analysis

2.5.1. UV-Vis Spectroscopy

Milli-Q ultrapure water was used as a blank. Absorbance measurements of HA, FA, and their complexes with PFBS and PFBA were taken using a UV-Vis spectrophotometer over a wavelength range of 200–800 nm with a 1 nm scanning interval.

2.5.2. Three-Dimensional Fluorescence Spectroscopy

Three-dimensional excitation-emission matrix (3D-EEM) fluorescence was measured by Hitachi F-7000 fluorophotometer (Hitachi, Shanghai, China). The excitation wavelength (Ex) ranged from 200 nm to 450 nm, with an increase of 5 nm, while the emission wavelength (Em) was between 280 and 550 nm, with an increase of 5 nm. The photomultiplier voltage was 700V, the scanning speed was 12,000 $nm \cdot min^{-1}$, and the slit width of both excitation monochromator and emission monochromator was 10 nm. Dilution of HA and FA solutions with Milli-Q water ensured absorbance remained below 0.3 at 254 nm to minimize inner filter effects. Parallel factor analysis (PARAFAC) was conducted to investigate the fluorescence components of humic substances in all samples.

2.5.3. FTIR Spectroscopy

For Fourier-transform infrared (FTIR) spectroscopy, 25 mL of humic substances filtrate was freeze-dried, and 1.0 mg of the resulting humic substances sample was mixed and homogenized with 200 mg of KBr (spectroscopic grade). The mixture was then pressed into pellets at 50–100 MPa and analyzed using an FTIR spectrometer (Spectrum 65, PerkinElmer, Waltham, MA, USA) over a wavenumber range of 4000–450 cm^{-1}, with a resolution of 4 cm^{-1} and 16 scans.

2.6. Complexation Models

The modified Stern–Volmer model (1) and site-specific complexation model (2) are commonly employed to characterize the complexation behavior of humic substances [9,10], and were used here to analyze the complexation constants and site numbers for interactions between humic substances and PFASs.

$$\frac{F_0}{F_0 - F} = \frac{1}{fK_{sv}[Q]} + \frac{1}{f} \quad (1)$$

$$log[F_0 - F/F] = logK_b + nlog[Q] \quad (2)$$

In these equations, F_0 and F represent the fluorescence intensities of humic substances in the absence and presence of PFASs, respectively. $[Q]$ denotes PFAS concentration (mol/L), K_{sv} is the Stern–Volmer constant, and f is the proportion of fluorescent sites bound to PFAS. K_b represents the complexation constant and n is the number of binding sites in the model.

2.7. Data Analysis

Data processing and calculations were performed in Microsoft Excel 2019, covering mean values, standard deviation (SD), relative standard deviation (RSD), and one-way analysis of variance (ANOVA), with a significance threshold set at $p = 0.05$. The 3D-EEM spectra and associated figure were generated using Origin 2021 software. PARAFAC were conducted using the removescatter and DOMfluor toolboxes in Matlab2018a.

Fluorescence data processing, including removal of Raman and Rayleigh scatter and normalization, was performed in Matlab R2009a, with PARAFAC applied to analyze fluorescence components [9,10]. SPSS was utilized for correlation analysis, principal component analysis, cluster analysis, and multiple linear regression, following methodologies from previous studies [11,12].

FTIR data were background-subtracted and processed with Omnic 8.0 software for baseline correction, smoothing, and normalization, and the resulting spectra were visualized in Origin 8.0. The Mantel test and graphical visualization were conducted using the linKEt package in RStudio. Redundancy analysis (RDA) was used to explore relationships between HA chemical diversity and PFAS complexation activity.

3. Results and Discussion

3.1. Analysis of Organic Matter Chemical Properties in Complexation and Adsorption Reactions

3.1.1. UV-Vis Spectral Characteristics

The chemical properties of humic substances following complexation and adsorption were evaluated using UV-Vis absorbance indices and fluorescence spectroscopy (Figure 1). Compared to D2PA, both D1PS and D1PA exhibited significantly higher SUVA_{254} and SUVA_{280} indices ($p < 0.05$), indicating a greater accumulation of humic substances and macromolecules following the HA complexation trials with PFBS and PFBA. However, no statistically significant difference was observed between D1PS and D2PS ($p > 0.05$), suggesting that although the concentration of humic substances and certain macromolecules in the HA test group was higher than that in the FA test group, the difference was not substantial.

Among the four experimental groups, the A_{250}/A_{365} ratio was significantly higher in the FA test groups than in the HA test groups ($p < 0.001$), indicating stronger hydrophobicity of HA samples. Similarly, the humification indices (HIX and HIXg) were also significantly higher in the HA test groups compared to the FA test groups ($p < 0.001$), suggesting a greater degree of humification in HA samples regardless of complexation with PFBS or PFBA. Compared with the HA group, the biological index (BIX) of the FA group was significantly higher ($p < 0.001$), which may be because the structure of FA is simpler and easier to degrade than that of HA. Therefore, the complexation of FA with PFBA and PFBS may produce a stronger fluorescence reaction and thus may show a higher BIX value.

After humic substances' complexation with PFBS and PFBA, the Total Organic Carbon (TOC) concentrations in the PFBA group was significantly higher than those in the PFBS group, likely due to differences in molecular structure, affinity, molecular size, diffusion, charge, solubility, as well as competitive adsorption and desorption between PFBA and PFBS [16]. These structural differences may affect their affinity with HA.

PFBA may interact more strongly with functional groups in HA (e.g., carboxyl groups), forming more stable complexes. PFBA's higher molecular diffusivity may facilitate frequent interactions with HA, resulting in greater organic carbon complex formation in aqueous samples. Additionally, the distinct charge characteristics of PFBA and PFBS may impact their solubility and interactions with HA. The negative charge of PFBA, as a carboxylic acid, may enhance its binding with negatively charged HA components. Given its weaker adsorption tendency, PFBA may be more readily displaced in competitive adsorption with HA, contributing to the higher TOC concentration.

The TOC concentration in the PFBA-FA complexation group was notably higher than in the HA-PFBS, HA-PFBA, and FA-PFBS groups. This could be attributed to differences in molecular weight among types of humic substances; FA, having a lower molecular weight, may form larger aggregates with PFBA, resulting in a higher TOC concentration. Additionally, FA contains more negatively charged functional groups, such as carboxyl groups, which may interact more strongly with PFBA to form stable complexes and increase TOC concentration.

Fluorescence index (FI) results showed that FI values in the FA complexation groups were significantly higher than those in the HA groups, likely due to FA's generally higher solubility, allowing it to contact and complex with more PFBA and PFBS molecules under similar conditions.

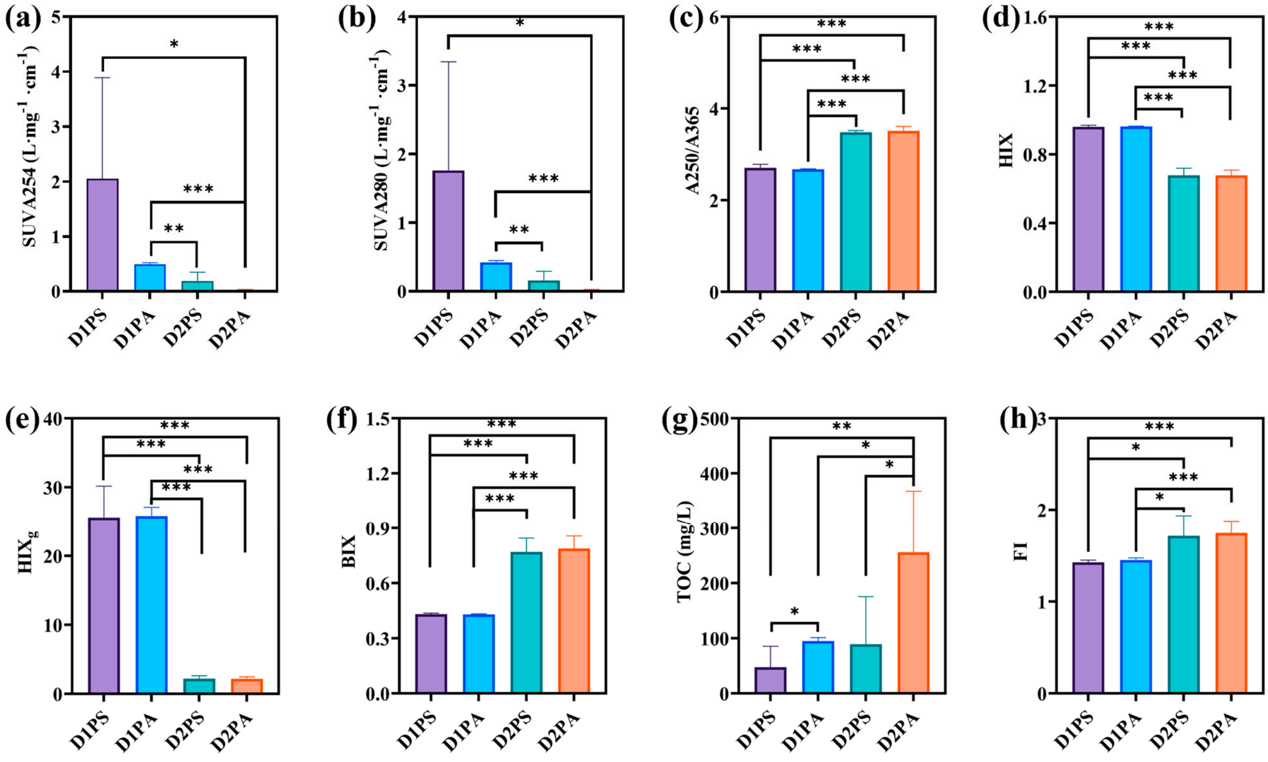

Figure 1. Chemical properties of humic substances revealed by SUVA254 (**a**), SUVA280 (**b**), A250/A365 (**c**), HIX (**d**), HIXg (**e**), BIX (**f**), TOC (**g**) and FI (**h**). The significance levels are as follows: *** $p < 0.001$, ** $p < 0.01$, * $p < 0.05$.

Environmental factors, such as pH and ionic strength, may also influence complexation efficiency. FA's greater flexibility and adaptability could contribute to a higher complexation capacity under varying environmental conditions. The greater number of carboxyl and phenolic hydroxyl groups in FA can interact strongly with fluorine atoms in PFBA and PFBS, potentially leading to a higher FI value. The electronegativity and spatial configuration of these functional groups may further facilitate complexation with PFBA and PFBS [17,18].

3.1.2. Fluorescence Component Characteristics

PARAFAC was conducted on 22 samples to investigate the fluorescence components of humic substances, classifying into two components (Figure 2a,b). Component 1 (C1, Ex/Em = 275, 375/445 nm) corresponds to HA, while Component 2 (C2, Ex/Em = 250/450 nm) corresponds to FA. Figure 2c,d indicate that the relative abundance of C1 in D1PS and D1PA samples was significantly higher than in D2PS and D2PA samples, whereas C2 was more abundant in the D2PS and D2PA samples. This is because 10 mg/L HA was added to the D1PS and D1PA groups, while 10 mg/L FA was added to the D2PS and D2PA groups.

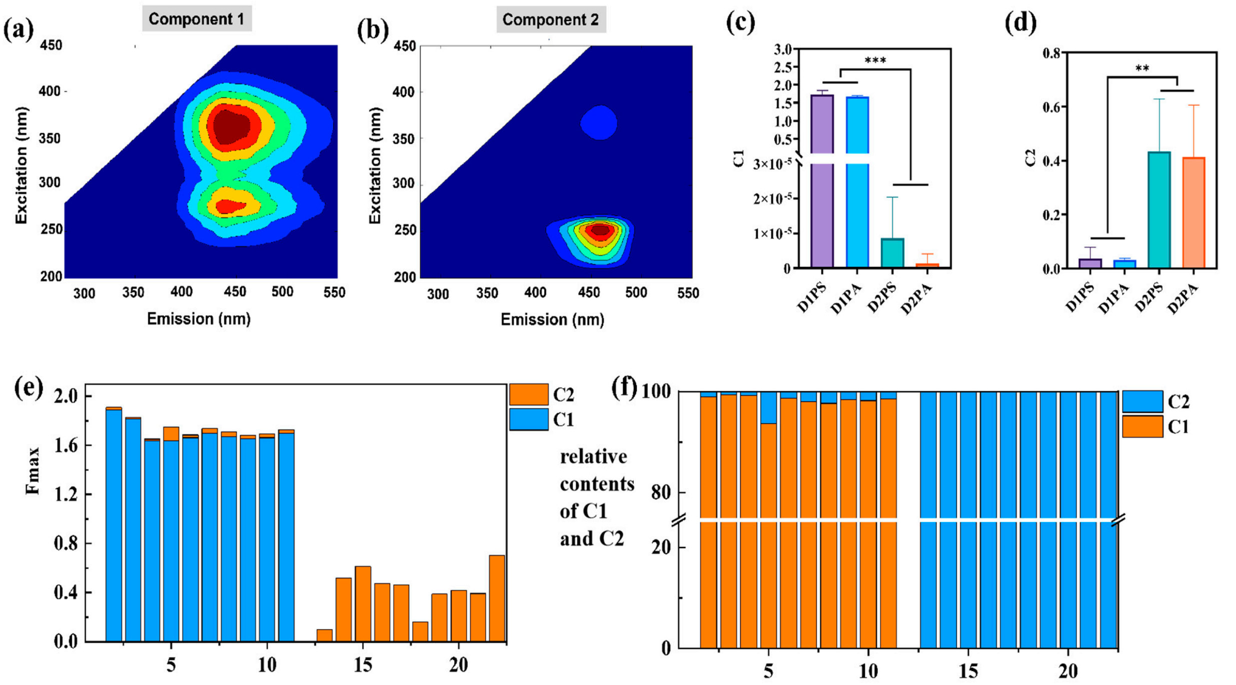

Figure 2. Fluorescence shapes of two components (C1 and C2) derived from PARAFAC-modeling (**a**,**b**), significant difference analysis of C1 and C2 (**c**,**d**), and Fmax and relative contents of C1 and C2 (**e**,**f**). The significance levels are as follows: *** $p < 0.001$, ** $p < 0.01$.

From Figure 2c–f, it can be observed that small amounts of FA were separated in samples with added HA, likely due to natural FA content in samples. Similarly, although small amounts of HA were detected in samples with added FA, the relative content was very low, likely due to the lower molecular weight of FA compared to HA. As a result, HA was mostly filtered out, while more FA remained.

Additionally, the fluorescence intensity (Fmax) values of the fluorescent components in the HA-PFBA and HA-PFBS complexation groups were significantly higher than those in the FA group. This could be attributed to the lower solubility of HA relative to FA, making the HA-PFBA and HA-PFBS complexes more resistant to hydrolysis or dispersion under the experimental conditions, resulting in higher fluorescence detection concentrations [19]. Furthermore, the complex molecular structure and relatively high molecular weight of the HA complexes with PFBA and PFBS may contribute to their enhanced stability, leading to higher concentrations of HA fluorescence components in the parallel factor analysis [20]. In landfill, the content of HA in landfill garbage and leachate will increase with the landfill time. When HA in landfill garbage migrates into leachate, PFBA and PFBS in landfill garbage may enter into leachate together with HA, because HA and their complex are stable. This means we need to focus on the risk of PFASs in leachate from aging landfills.

The strong fluorescence properties of HA may be due to its conjugated systems and aromatic rings, which enhance its ability to absorb and emit light energy effectively when complexed with PFBA and PFBS [21]. This structural composition allows HA to display stronger fluorescence characteristics, providing additional insight into its interactions with PFAS compounds.

3.1.3. FTIR Spectral Characteristics

The molecular characteristics of humic substances were analyzed using Fourier-transform infrared spectroscopy (FTIR) (Figure 3). Figure 3a,b display the FTIR spectra of all samples from the HA complexation experiments with PFBA and PFBS. The molecular structure of HA includes aromatic rings, heterocyclic and polycyclic compounds connected by carbon chains or bridges, forming a loose network. Functional groups such as carboxyl, phenolic hydroxyl, methoxy, and amide groups are located at the edges of the HA molecules, which influence their acidity, adsorption capacity, and ability to form organo-mineral complexes with inorganic substances.

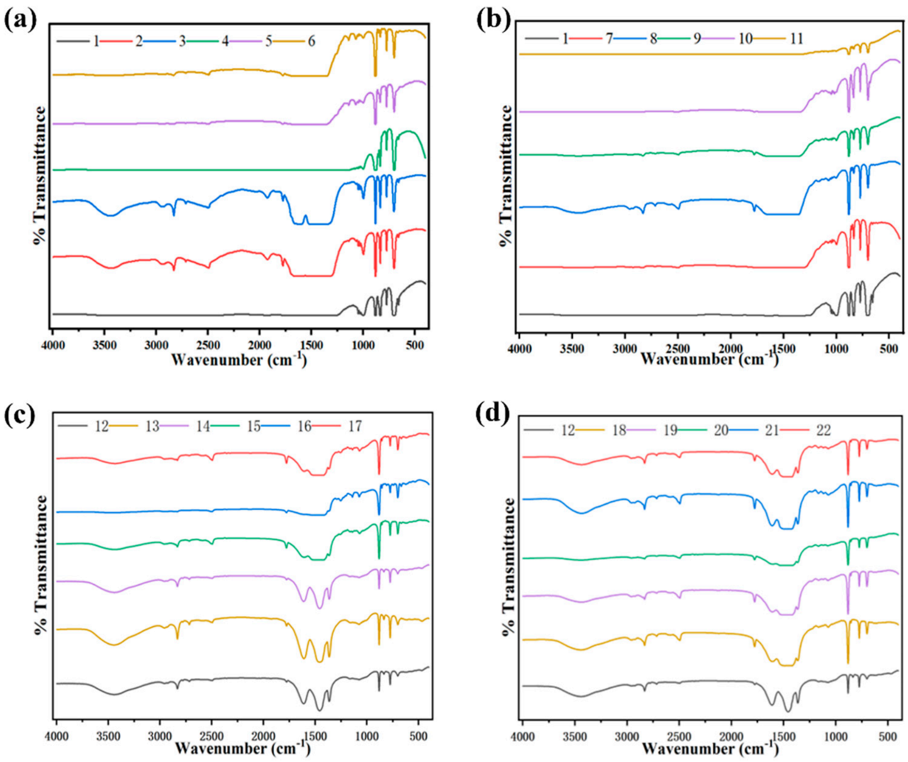

Figure 3. Characteristics of humic substances and PFASs: (**a**) the test group of HA and PFBS; (**b**) the test group of HA and PFBA; (**c**) the group of FA and PFBS; and (**d**) the test group of FA and PFBA. Sample information corresponding to numbers 1–22 is shown in Table S2.

In Figure 3a,b, all samples show strong peaks between 873 and 692 cm^{-1}, corresponding to C-O and CH_2 bending vibrations [22], which are primarily associated with oxygen-containing functional groups and CH_2 vibrations in aliphatic structures. This indicates that the complexation samples of HA contain high levels of oxygen-containing functional groups and alkanes. The absorption peaks in this range were strong across all concentrations of PFBS complexed with HA, whereas in the HA-PFBA complexation experiment, the 100 μmol/L PFBA sample (D1PA Sample 5) exhibited a weaker absorption peak in this range. This suggests that, at higher concentrations of PFBA, the functional groups primarily involved in complexation with HA are C-O and CH_2.

Figure 3c,d show the FTIR spectra for all samples from the FA complexation experiments with PFBA and PFBS. The molecular structure of FA contains multiple ring structures, primarily composed of benzene and benzoic acid rings that form a complex, highly polar network through hydrogen bonding. This unique network structure enables FA to bind with organic and inorganic substances via hydrogen bonding, ion exchange, charge transfer, complexation, and chemical adsorption mechanisms [23].

Figure 3c,d reveal peaks between 2720 and 2830 cm^{-1}, indicating the presence of aldehyde groups, and peaks between 1680 and 1750 cm^{-1}, suggesting the presence of carbonyl groups. The peak at 3400 cm^{-1} is attributed to O-H stretching in humic substances. For samples 16 and 20, the peak at 3400 cm^{-1} is weakened, suggesting a reduction in hydroxyl groups when FA is complexed with 75 μmol/L PFBS and 50 μmol/L PFBA. This decrease may result from the preferential complexation of FA hydroxyl groups with PFBS and PFBA at these concentrations.

The peak at 1648 cm^{-1} signifies an accumulation of amides, quinones, ketones, and other aromatic compounds. In the FTIR spectra of samples 16 and 20, the peak at 1648 cm^{-1} is notably weakened, indicating that in addition to hydroxyl groups, amide, quinone, and ketone functional groups participate in complexation with PFBS and PFBA. Amide groups, as nitrogen-containing functional groups, likely contribute to hydrogen bonding and other intermolecular interactions.

3.2. Analysis of Complexation and Adsorption Between Humic Substances and PFASs

The spectral results above indicate that the introduction of PFASs alters the chemical diversity of organic matter in humic substances, suggesting that PFASs may significantly influence humic substances' complexation behavior, thereby affecting the environmental transport, fate, and risk profile of PFASs. Previous studies have shown that the chemical diversity of humic substances is a critical factor in modulating its complexation activity in the environment [24,25]. A Circos plot was used to identify and summarize differences in humic substances chemical diversity across samples (Figure 4). In samples D1PS and D1PA, darker lines and larger intervals were observed in $SUVA_{254}$, $SUVA_{280}$, and HIXg, indicating a higher content of aromatic compounds.

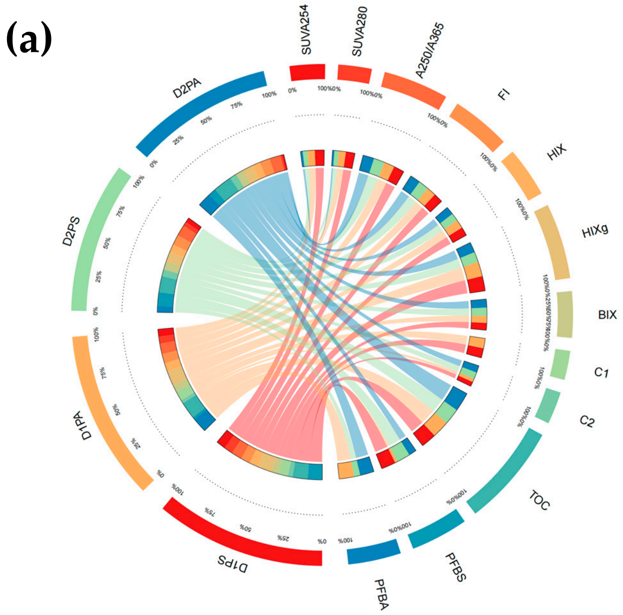

Figure 4. *Cont.*

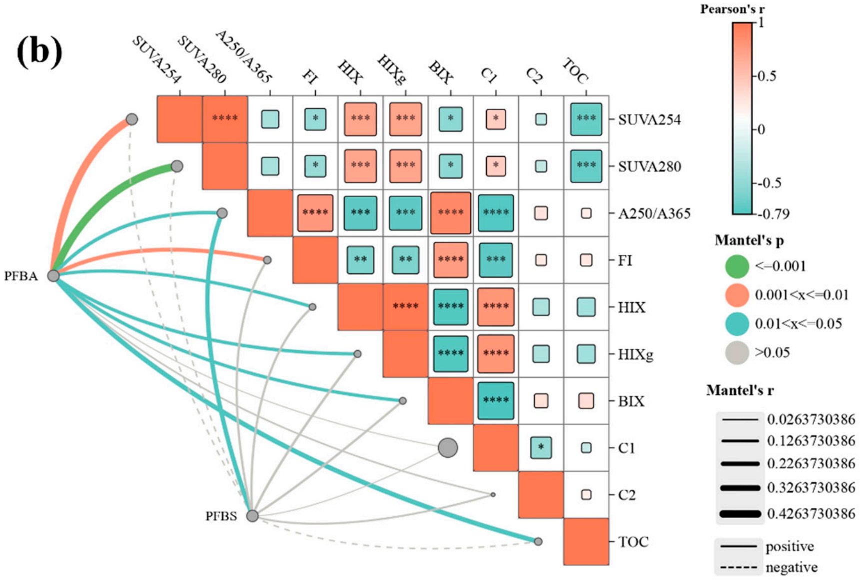

Figure 4. Correlation plot of each component after complexation of humic substances and PFASs ((**a**) for Circos, (**b**) for Mantel). The significance levels are as follows: **** $p < 0.0001$, *** $p < 0.001$, ** $p < 0.01$, * $p < 0.05$.

Based on the chemical diversity of humic substances in leachate and the polar–nonpolar duality of PFASs, we hypothesize that humic substances in leachate may form complexes with PFASs through both specific and non-specific interactions. For example, hydrophobic interactions may occur between the benzene rings in PFASs and humic substances. Hydrogen bonding or ligand exchange may occur between the carboxyl groups of PFASs and polar functional groups in humic substances (e.g., amino, hydroxyl, and carboxyl groups). Electrostatic and van der Waals interactions may arise between electron-withdrawing groups in PFASs (e.g., carboxyl or sulfonic acid groups) and electron-donating groups in humic substances.

3.2.1. Analysis of Organic Matter Complexation and Adsorption Activity

Fluorescence quenching experiments were conducted with PFASs as the quencher to evaluate the complexation activity of humic substances. With increasing PFAS concentrations, the Fmax of all samples decreased, indicating complex interactions that likely altered the structure of humic substances [24]. Previous studies have shown that the toxicity and mobility of pollutants are influenced by their molecular structure [26,27]. Consequently, the complexation interactions between PFASs and humic substances may indirectly impact the environmental transport and risks.

To further explore the complex characteristics of humic substances and PFAS interactions, the Stern–Volmer equation was used to fit the dataset. As shown in Table S3, the complexation behavior of humic substances aligns well with the Stern–Volmer equation, with R^2 values ranging from 0.763 to 0.992, and it also fits well with the site-specific complexation model, with R^2 values from 0.703 to 0.993.

The binding constant ($logK_{sv}$) for the interaction between humic substances and PFASs ranged from 1.066 to 1.684. For PFBS, the $logK_{sv}$ of D1PS was greater than that of D2PS; similarly, for PFBA, the $logK_{sv}$ of D1PA was greater than that of D2PA. This indicates that HA forms stronger, more stable interactions with both PFBS and PFBA [27,28]. However, for the binding constant $logK_b$, D2PS exhibited a significantly higher $logK_b$ than D1PS, which is inconsistent with the findings for $logK_{sv}$. This suggests that the complexation behavior of humic substances varies depending on the target contaminant, and that the interactions between humic substances and PFASs may involve unique mechanisms.

Since the complexation activity of humic substances largely depends on its chemical diversity [24,25], redundancy analysis (RDA) was conducted to investigate the relationship between humic substances chemical diversity and PFAS complexation activity (Figure 5). Samples D1PA and D1PS exhibited higher $logK_{sv}$ and $logK_b$ values, which positively correlated with $SUVA_{254}$, HIX, HIXg, and Component 1 (C1), while showing a negative correlation with TOC, BIX, FI, A_{250}/A_{365}, and Component 2 (C2). In contrast, samples D2PA and D2PS were positively correlated with TOC, BIX, FI, A_{250}/A_{365}, and C2, and negatively correlated with HIX and $SUVA_{254}$. These correlations indicate that D1PA and D1PS contain larger molecular weights, and higher aromaticity, whereas D2PA and D2PS demonstrate stronger complexation capacities, consistent with findings for MCPA, atrazine, and antibiotics [9,27,29].

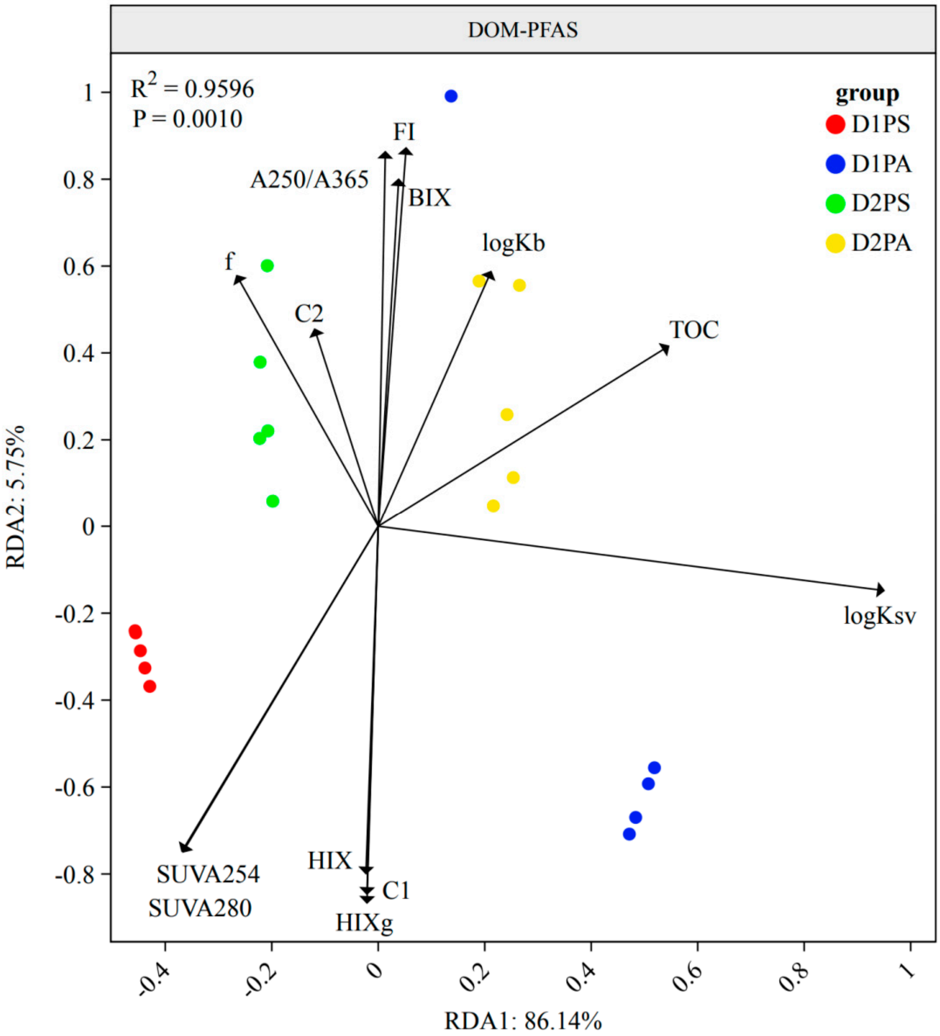

Figure 5. Redundancy analysis diagram of the chemical characteristics of humic substances and the complexation parameters of humic substances with PFASs.

Some researchers have noted that the binding activity of humic substances for nonpolar pollutants (e.g., polycyclic aromatic hydrocarbons) is primarily positively correlated with humic substances' molecular weight, aromaticity, and hydrophobicity, rather than being influenced by polar functional groups [27,30,31]. These results suggest that the complexation behavior of humic substances varies by target pollutant, and that humic substances' interactions with PFASs may involve unique mechanism.

3.2.2. Identification of Organic Components in Complexation and Adsorption Reactions

To further identify the key components in the interaction between humic substances and PFASs, parallel factor analysis was applied to the three-dimensional fluorescence quenching data of humic substances. As shown in Figure 6, the quenching curves vary significantly depending on the type of humic substances and the fluorescence component. For D2PS samples, slight increases and fluctuations in Fmax values were observed in the quenching curve, suggesting a lower stability of the complexation reaction. A previous study similarly noted that Zn(II) negatively affected the fluorescence quenching of humic substances due to low complexation stability [28]. Other potential causes of negative quenching effects include PFASs displacing the original quenching agents of humic substances, thus altering humic substances' fluorescence structure and quantum yield [24].

Overall, the Fmax values of D1PS and D1PA samples decreased with increasing PFAS concentrations. This suggests that HA (C1) plays a more significant role in the complexation process compared to FA. For D1PS samples, as the PFBS concentration increased, the Fmax value decreased by 13.28%. These results align with the fits obtained from the Stern–Volmer and Ryan–Weber equations, indicating that D1PS had higher $logK_{sv}$ and $logK_b$ values than the other two components. Additionally, the value of n was highest in D1PS, suggesting more binding sites in HA [32].

The differences in the complexation activity and binding sites of fluorescence components may also relate to humic substances' chemical properties. The Mantel test results indicate a positive correlation between HA (C1) and HIX and HIXg (Figure 6b). Furthermore, the correlation with FA (C2) was lower than that with HA (C1), underscoring the higher aromaticity of humic substances in C1. Previous studies have found that fluoroquinolone antibiotics (FQS) and 2,4-dichlorophenoxyacetic acid (MCPA) can interact with polar groups such as O-H, C-H, and -COOH in humic substances via van der Waals forces, hydrogen bonding, and electrostatic effects [32]. Consequently, it can be concluded that high aromaticity is a prerequisite for humic substances and PFAS interactions, with polar functional groups serving as favorable factors.

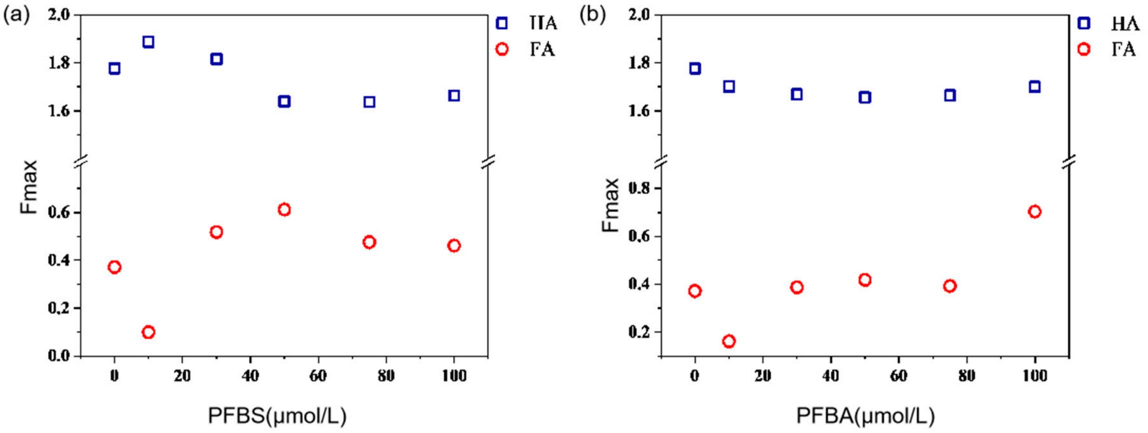

Figure 6. Quenching curves of humic substances interacting with PFBS (**a**), and with PFBA (**b**).

3.2.3. Molecular-Level Analysis of Complexation and Adsorption Mechanisms

To further elucidate the mechanisms underlying humic substances and PFAS complexation, UV-Vis absorption and FTIR spectroscopy were employed. Humic substance complexation with quenchers typically involves two primary quenching mechanisms: static quenching, which arises from the binding of the quencher to the fluorophore, and dynamic quenching, resulting from collisions between the quencher and the fluorophore in the excited state [32]. As shown in Figure 1a–c, the UV-Vis absorbance of humic substances decreased progressively with the addition of PFBS and PFBA. This observation suggests that PFASs' presence can alter the humic substances' structure and form complexes with humic substances [33], consistent with the fluorescence spectroscopy results (Figure 2).

To further investigate the molecular mechanisms of humic substances and PFAS interactions, FTIR spectroscopy was applied to characterize humic substances and PFAS complexes (Figure 3). As PFAS concentrations increased, the intensity of FTIR peaks decreased, particularly at 1401, 1648, 1680–1750, and 2720–2830 cm^{-1}. This indicates that humic substances interact with PFASs through a complex interplay of hydrophobic interactions, ligand exchange, hydrogen bonding, π-π interactions, and van der Waals forces involving functional groups such as hydroxyl (O-H), aliphatic CHx, aromatic C=C, amides, quinones, and ketones. These findings align with our hypothesis that humic substances exhibit specific, complex interactions with PFASs that differ from its interactions with non-polar pollutants.

Research suggests that non-polar pollutants (e.g., polycyclic aromatic hydrocarbons) primarily interact with humic substances via electron dipole–dipole forces, such as π-π interactions and hydrophobic interactions. The chemical differences between PFASs and non-polar pollutants may explain this phenomenon. Unlike non-polar pollutants with solely aromatic structures, PFASs are surfactants containing additional polar carboxyl or sulfonic acid groups. Therefore, humic substances can form complexes with PFASs through non-specific interactions among benzene rings as well as specific interactions among polar functional groups [33].

4. Conclusions and Recommendations

This study investigated the complexation mechanisms between humic substances and PFASs in landfill leachate at the molecular level. The findings revealed that after complexation and adsorption, HA exhibits high aromaticity; FA, which has better solubility than HA, readily forms complexes with PFBA and PFBS. When complexed with 100 μmol/L PFBA, the primary functional groups in HA were C-O and CH_2; in the complexation of 75 μmol/L PFBS and 50 μmol/L PFBA with FA, hydroxyl groups were predominant. The complexation and adsorption of humic substances with PFASs showed that the $logK_{sv}$ and $logK_b$ values were higher in HA samples, correlating positively with C1, C2, $SUVA_{254}$, A_{250}/A_{365}, HIX, HIXg, and FI, and negatively with BIX. This suggests that HA engages in more complex and stable interactions with PFBS and PFBA. Humic substance complexation with PFASs involves a range of forces, including hydrophobic interactions, van der Waals forces, hydrogen bonds, ionic bonds, and covalent bonds, through hydroxyl (O-H), aliphatic CHx, aromatic C=C, amide, quinone, and ketone groups.

The leachate contains not only a large amount of DOM but also numerous inorganic salts, heavy metals, and microorganisms, which may influence the DOM-PFAS complexation process. Therefore, the complexation of DOM and PFASs in a real leachate environment is more intricate. In future studies, in addition to exploring the DOM-PFAS complexation, it is important to investigate the impact of other environmental factors on their interactions.

The results demonstrated that PFASs is an important group of characteristic contaminants in landfill leachate. The remediation and environmental risk control policy for landfill leachate should focus on PFASs as well as DOM, and other contaminants. Enhanced co-regulation and mitigation strategies addressing the combined pollution of PFASs and DOM in landfill leachate will be highly demanded in future practices. The mitigation techniques for the combined pollution of PFASs and DOM should consider the complexation and adsorption mechanisms at the molecular level.

Future efforts should focus on strengthening the environmental risk management of PFASs in landfill leachate, particularly by enhancing collaborative controls for PFASs and humic substances. Firstly, source prevention should be prioritized, as the 16 landfills in the study area are situated in aquifer systems with porous, loose rock formations. Landfills like BJH, BJD, ZZ, SH, and DCha are located in areas with high groundwater abundance, where measures should be implemented to assess the integrity of impermeable layers, monitor leakage detection layers, and evaluate the effectiveness of containment systems.

Secondly, PFAS management and risk control in leachate should be enhanced, such as by upgrading landfill leachate treatment technologies to improve PFAS remediation effectiveness. PFASs should be considered a characteristic pollutant in landfills, prompting detailed groundwater environmental investigation and implementing pollution control and remediation measures as needed.

Lastly, continuous monitoring of PFASs in groundwater is crucial. Municipal solid waste landfills should establish groundwater quality monitoring wells as legally required, incorporating PFASs as a monitoring factor in groundwater assessment programs.

Supplementary Materials: The following supporting information can be downloaded at: https://www.mdpi.com/article/10.3390/w16233527/s1, Table S1: Information of 16 landfill sites in the studied area; Table S2: Fluorescence-quenching titration experiment between humic substances and PFAS; Table S3: Table of parameters for the complexation models.

Author Contributions: J.L.: Writing of the original draft, writing—review and editing, methodology, investigation, formal analysis, and visualization. H.S.: Writing of the original draft, methodology, investigation, and software. R.Y.: Formal analysis and visualization. P.Z.: Formal analysis and methodology. S.C.: Investigation and software. G.Z.: Methodology and visualization, writing—review and editing. W.T.: Formal analysis, methodology, visualization, and supervision. All authors have read and agreed to the published version of the manuscript.

Funding: This research was funded by the National Natural Science Foundation of China (No. 42030704) and the National Key Research and Development Program of China (No. 2023YFC3707703).

Data Availability Statement: Data will be made available on request. The data presented in this study are available on request from the corresponding author. The data are not publicly available due to privacy restrictions.

Conflicts of Interest: The authors declare that they have no known competing financial interests or personal relationships that could have appeared to influence the work reported in this manuscript.

References

1. Ackerman Grunfeld, D.; Gilbert, D.; Hou, J.; Jones, A.M.; Lee, M.J.; Kibbey, T.C.; O'Carroll, D.M. Underestimated burden of per-and polyfluoroalkyl substances in global surface waters and groundwaters. *Nat. Geosci.* **2024**, *17*, 340–346. [CrossRef]
2. Evich, M.G.; Davis, M.J.B.; Mccord, J.P.; Acrey, B.; Awkerman, J.A.; Knappe, D.R.U.; Lindstrom, A.B.; Speth, T.F.; Tebes-Stevens, C.; Strynar, M.J.; et al. Per-and polyfluoroalkyl substances in the environment. *Science* **2022**, *375*, eabg9065. [CrossRef]
3. Hamid, H.; Li, L.Y.; Grace, J.R. Review of the fate and transformation of per- and polyfluoroalkyl substances (PFASs) in landfills. *Environ. Pollut.* **2018**, *235*, 74–84. [CrossRef]
4. Liu, T.; Hu, L.-X.; Han, Y.; Dong, L.-L.; Wang, Y.-Q.; Zhao, J.-H.; Liu, Y.-S.; Zhao, J.-L.; Ying, G.-G. Non-target and target screening of per- and polyfluoroalkyl substances in landfill leachate and impact on groundwater in Guangzhou, China. *Sci. Total Environ.* **2022**, *844*, 157021. [CrossRef]
5. Wang, F.; Liu, W.; Jin, Y.; Dai, J.; Zhao, H.; Xie, Q.; Liu, X.; Yu, W.; Ma, J. Interaction of PFOS and BDE-47 Co-exposure on Thyroid Hormone Levels and TH-Related Gene and Protein Expression in Developing Rat Brains. *Toxicol. Sci.* **2011**, *121*, 279. [CrossRef]
6. Whitacre, D.M.; Giesy, J.P.; Naile, J.E.; Khim, J.S.; Jones, P.D.; Newsted, J.L. *Aquatic Toxicology of Perfluorinated Chemicals*; Springer: Berlin/Heidelberg, Germany, 2010.
7. Qazi, M.R.; Abedi, M.R.; Nelson, B.D.; DePierre, J.W.; Abedi-Valugerdi, M. Dietary exposure to perfluorooctanoate or perfluorooctane sulfonate induces hypertrophy in centrilobular hepatocytes and alters the hepatic immune status in mice. *Int. Immunopharmacol.* **2010**, *10*, 1420–1427. [CrossRef]
8. Kim, M.; Son, J.; Park, M.S.; Ji, Y.; Chae, S.; Jun, C.; Bae, J.-S.; Kwon, T.K.; Choo, Y.-S.; Yoon, H.; et al. In vivo evaluation and comparison of developmental toxicity and teratogenicity of perfluoroalkyl compounds using Xenopus embryos. *Chemosphere* **2013**, *93*, 1153–1160. [CrossRef]
9. Eggen, T.; Moeder, M.; Arukwe, A. Municipal landfill leachates: A significant source for new and emerging pollutants. *Sci. Total Environ.* **2010**, *408*, 5147–5157. [CrossRef]
10. Lang, J.R.; Allred, B.M.; Field, J.A.; Levis, J.W.; Barlaz, M.A. National Estimate of Per- and Polyfluoroalkyl Substance (PFAS) Release to U.S. Municipal Landfill Leachate. *Environ. Sci. Technol.* **2017**, *51*, 2197–2205. [CrossRef]
11. Slack, R.J.; Gronow, J.R.; Voulvoulis, N. Household hazardous waste in municipal landfills: Contaminants in leachate. *Sci. Total Environ.* **2005**, *337*, 119–137. [CrossRef]
12. Matejczyk, M.; Płaza, G.A.; Nałęcz-Jawecki, G.; Ulfig, K.; Markowska-Szczupak, A. Estimation of the environmental risk posed by landfills using chemical, microbiological and ecotoxicological testing of leachates. *Chemosphere* **2011**, *82*, 1017–1023. [CrossRef]
13. He, P.J.; Xue, J.F.; Shao, L.M.; Li, G.J.; Lee, D.J. Dissolved organic matter (DOM) in recycled leachate of bioreactor landfill. *Water Res.* **2006**, *40*, 1465–1473. [CrossRef]
14. Guo, X.; Tu, B.; Ge, J.; Yang, C.; Song, X.; Dang, Z. Sorption of tylosin and sulfamethazine on solid humic acid. *J. Environ. Sci.* **2016**, *43*, 208–215. [CrossRef]
15. Mei, W.; Sun, H.; Song, M.; Jiang, L.; Li, Y.; Lu, W.; Ying, G.-G.; Luo, C.; Zhang, G. Per- and polyfluoroalkyl substances (PFASs) in the soil–plant system: Sorption, root uptake, and translocation. *Environ. Int.* **2021**, *156*, 106642. [CrossRef]

16. Park MinKyu, P.M.; Wu ShiMin, W.S.; Lopez, I.J.; Chang, J.Y.; Karanfil, T.; Snyder, S.A. Adsorption of perfluoroalkyl substances (PFAS) in groundwater by granular activated carbons: Roles of hydrophobicity of PFAS and carbon characteristics. *Water Res.* **2020**, *170*, 115364. [CrossRef]
17. Patterson, H.H.; Cronan, C.S.; Lakshman, S.; Plankey, B.J.; Taylor, T.A. Comparison of soil fulvic acids using synchronous scan fluorescence spectroscopy, FTIR, titration and metal complexation kinetics. *Sci. Total Environ.* **1992**, *113*, 179–196. [CrossRef]
18. Amirbahman, A.; Olson, T.M. Transport of humic matter-coated hematite in packed beds. *Environ. Sci. Technol.* **1993**, *27*, 2807–2813. [CrossRef]
19. Su, Y.; Hu, E.; Feng, M.; Zhang, Y.; Chen, F.; Liu, Z. Comparison of bacterial growth in response to photodegraded terrestrial chromophoric dissolved organic matter in two lakes. *Sci. Total Environ.* **2017**, *579*, 1203–1214. [CrossRef]
20. Rodr Guez, F.J.; Schlenger, P.; Garc A-Valverde, M. A comprehensive structural evaluation of humic substances using several fluorescence techniques before and after ozonation. Part I: Structural characterization of humic substances. *Sci. Total Environ.* **2014**, *476*, 718–730. [CrossRef]
21. Miano, T.; Senesi, N. Synchronous excitation fluorescence spectroscopy applied to soil humic substances chemistry. *Sci. Total Environ.* **1992**, *117*, 41–51. [CrossRef]
22. Teng, Y.; Zhou, Q. Adsorption behavior of Sudan I-IV on a coastal soil and their forecasted biogeochemical cycles. *Environ. Sci. Pollut. Res. Int.* **2017**, *24*, 10749–10758. [CrossRef]
23. Reemtsma, T.; These, A.; Springer, A.; Linscheid, M. Fulvic acids as transition state of organic matter: Indications from high resolution mass spectrometry. *Environ. Sci. Technol.* **2006**, *40*, 5839–5845. [CrossRef]
24. Lee, S.C.; Shin, Y.; Jeon, Y.J.; Lee, E.J.; Eom, J.S.; Kim, B.; Oh, N.H. Optical properties and 14C ages of stream DOM from agricultural and forest watersheds during storms. *Environ. Pollut.* **2021**, *272*, 116412. [CrossRef]
25. Wang, M.; Chen, Y. Generation and characterization of DOM in wastewater treatment processes. *Chemosphere* **2018**, *201*, 96–109. [CrossRef]
26. Ren, G.; Wang, X.; Zhang, Z.; Zhong, B.; Yang, L.; Xu, D.; Yang, X. Facile synthesis of maghemite nanoparticle from waste green vitriol as adsorbent for adsorption of arsenite. *J. Mol. Liq.* **2018**, *259*, 32–39. [CrossRef]
27. Wu, D.; Ren, D.; Li, Q.; Zhu, A.; Song, Y.; Yin, W.; Wu, C. Molecular linkages between chemodiversity and MCPA complexation behavior of dissolved organic matter in paddy soil: Effects of land conversion. *Environ. Pollut.* **2022**, *311*, 119949. [CrossRef]
28. Guo, F.; Qin, S.; Xu, L.; Bai, Y.; Xing, B. Thermal degradation features of soil humic acid sub-fractions in pyrolytic treatment and their relation to molecular signatures. *Sci. Total Environ.* **2020**, *749*, 142318. [CrossRef]
29. Zhu, L.-J.; Zhao, Y.; Chen, Y.-N.; Cui, H.-Y.; Wei, Y.-Q.; Liu, H.-L.; Chen, X.-M.; Wei, Z.-M. Characterization of atrazine binding to dissolved organic matter of soil under different types of land use. *Ecotoxicol. Environ. Saf.* **2018**, *147*, 1065–1072. [CrossRef]
30. Polubesova, T.; Sherman-Nakache, M.; Chefetz, B. Binding of pyrene to hydrophobic fractions of dissolved organic matter: Effect of polyvalent metal complexation. *Environ. Sci. Technol.* **2007**, *41*, 5389–5394. [CrossRef]
31. Wang, H.; Zhang, Y. Mechanisms of interaction between polycyclic aromatic hydrocarbons and dissolved organic matter. *J. Environ. Sci Health A Tox Hazard. Subst. Environ. Eng.* **2014**, *49*, 78–84. [CrossRef]
32. Wang, L.; Wu, X.; Zhao, Z.; Fan, F.; Zhu, M.; Wang, Y.; Na, R.; Li, Q.X. Interactions between imidacloprid and thiamethoxam and dissolved organic matter characterized by two-dimensional correlation spectroscopy analysis, molecular modeling, and density functional theory calculations. *J. Agric. Food Chem.* **2020**, *68*, 2329–2339. [CrossRef] [PubMed]
33. Qi, Y.; Cao, H.; Pan, W.; Wang, C.; Liang, Y. The role of dissolved organic matter during Per- and Polyfluorinated Substance (PFAS) adsorption, degradation, and plant uptake: A review. *J. Hazard. Mater.* **2022**, *436*, 129139. [CrossRef] [PubMed]